ACS APPLIED MATERIALS & INTERFACES

Research Article

www.acsami.org

Substrate Stiffness Regulates the Development of Left−Right Asymmetry in Cell Orientation

Yuanye Bao,[†] Yaozhun Huang,[†] Miu Ling Lam,[*,‡,§,#] Ting Xu,[†] Ninghao Zhu,[†] Zhaobin Guo,[†] Xin Cui,[†] Raymond H. W. Lam,[†,§,#] and Ting-Hsuan Chen[*,†,‡,§,#]

[†]Department of Mechanical and Biomedical Engineering, [‡]School of Creative Media, and [§]Centre for Robotics and Automation, City University of Hong Kong, 83 Tat Chee Avenue, Hong Kong Special Administrative Region, China

[#]CityU Shenzhen Research Institute, Shenzhen 518057, China

Supporting Information

ABSTRACT: Left−right (LR) asymmetry of tissue/organ structure is a morphological feature essential for many tissue functions. The ability to incorporate the LR formation in constructing tissue/organ replacement is important for recapturing the inherent tissue structure and functions. However, how LR asymmetry is formed remains largely underdetermined, which creates significant hurdles to reproduce and regulate the formation of LR asymmetry in an engineering context. Here, we report substrate rigidity functioning as an effective switch that turns on the development of LR asymmetry. Using micropatterned cell-adherent stripes on rigid substrates, we found that cells collectively oriented at a LR-biased angle relative to the stripe boundary. This LR asymmetry was initiated by a LR-biased migration of cells at stripe boundary, which later generated a velocity gradient propagating from stripe boundary to the center. After a series of cell translocations and rotations, ultimately, an LR-biased cell orientation within the micropatterned stripe was formed. Importantly, this initiation and propagation of LR asymmetry was observed only on rigid but not on soft substrates, suggesting that the LR asymmetry was regulated by rigid substrate probably through the organization of actin cytoskeleton. Together, we demonstrated substrate rigidity as a determinant factor that mediates the self-organizing LR asymmetry being unfolded from single cells to multicellular organization. More broadly, we anticipate that our findings would pave the way for rebuilding artificial tissue constructs with inherent LR asymmetry in the future.

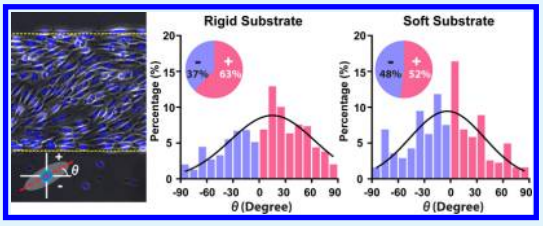

KEYWORDS: *stiffness, micropatterning, left−right asymmetry, cell chirality, cell orientation, migration*

1. INTRODUCTION

Left−right (LR) asymmetry is an architectural feature in animal bodies,[1−3] e.g., visceral distribution or internal structures of an organ, and is closely related to many tissue functions. For example, in a heart, the proper contractility of heart muscles requires the cardiac fibers assembling into layers of myocardium with specific orientation angles.[4] Errors in LR asymmetry may cause congenital diseases and failure of organ functions. Thus, it is crucially important to understand how LR asymmetry is formed such that it can be incorporated in healing or rebuilding ill-patterned tissues/organs to recapture the inherent tissue structures and functions. Recent reports suggest that LR asymmetry may be originated from individual cells with LR-biased mechanics, e.g., neutrophils' leftward migration,[5] blastomeres' uneven distribution,[6] rotation of *Xenopus* egg cortex,[7] and cell alignment on micropatterned substrate.[8−11] Likely, such activities are initially self-organized through the intrinsic behaviors of individual cells. During the developmental process, the LR bias of single cells is integrated and amplified, eventually leading to the LR asymmetry at tissue-level architectures.[9,11,12] However, how to reproduce and regulate the formation of LR asymmetry in an engineering context remains greatly unknown.

It has been noted that biophysical properties are essential for the expression of LR asymmetry. Actomyosin activities have been reported important for LR formation in early embryonic development,[6,7] cardiac looping,[13] and organ laterality.[14,15] More specifically, at the single cell level, the organization of actin stress fibers also determines the LR bias of cell chiral rotation[16] and migration.[8,9] Because actomyosin activities are coupled with physical environment surrounding cells, the extracellular mechanical factors, such as substrate stiffness, stretching force, and shear stress,[17−20] may also play important roles that mediate the expression and propagation of LR asymmetry.

Among many biophysical factors, substrate stiffness can affect various cell behaviors, including adhesion,[21] migration,[22] proliferation,[18] and differentiation.[23−26] Furthermore, it has been well proven that substrate stiffness can also mediate the subcellular cytoskeletal remodeling such as actomyosin-mediated contractility[27] and focal adhesion assembly.[28,29] For instance, when cultured on stiffer substrates, adherent cells

Received: June 7, 2016
Accepted: June 30, 2016

DOI: 10.1021/acsami.6b06789
ACS Appl. Mater. Interfaces XXXX, XXX, XXX−XXX

generally express reinforced contractile forces[27−29] and vice versa. Considering that substrate stiffness induces coupled effects on both actomyosin activity and cytoskeletal remodeling, very likely, the LR bias of cell motion is also dependent on substrate stiffness.

Here, we report that the formation of LR asymmetry can be turned on or off depending on substrate stiffness. Using micropatterned stripes of cell-adherent molecules on substrates with a range of stiffness, we investigated the expression of LR asymmetry by examining the cell orientation relative to the stripe boundary. The initiation and propagation of LR asymmetry were evaluated by LR-biased cell polarity and velocity gradient of cell migration, and the dynamics of cell orientation was investigated by means of time-lapsed microscopy and numerical simulation. Together, this research reveals the key roles of substrate stiffness in regulating the formation LR asymmetry. More broadly, we postulate that our findings provide important insights for reconstitution of *de novo* LR asymmetry, paving ways for rebuilding artificial tissue constructs with inherent LR asymmetry in the future.

2. EXPERIMENTAL SECTION

Micropatterning on Substrate with Varied Stiffness. Cell-adherent regions were micropatterned as stripes with width of 300 μm or circular islands with area of 3000 μm^2. By using polydimethylsiloxane (PDMS; Dow Corning) as the "soft substrate", we first cleaned and spin-coated 100 μm thick of PDMS (elastomer: cross-linker = 30:1) at 1000 rpm for 30 s on glass slides, followed by baking at 70 °C for 4 h. After applying a 2 min oxygen plasma treatment (800 mTorr, 30 W), we coated hexamethyldisilazane (HMDS, Sigma) on the PDMS. AZ5214 photoresist (PR, AZ Electronic Materials) was then spin-coated on the HMDS/PDMS surface at 3000 rpm and baked for 2 min at 95 °C. Next, UV exposure and development (AZ400 K, 1:2 dilution with deionized water, AZ Electronic Materials) were conducted to obtain the micropatterned stripes. Afterward, a 10 μg/mL fibronectin (FN; Life Technology) solution was coated on the stripes with exposed PDMS for 30 min. To remove the remaining PR and create cell-repellent surface, the substrate was washed with absolute ethanol for 5 min by 3 times, followed by applying 1−2% pluronic F127 (Sigma) in deionized water for 50 min to coat the exposed HMDS/PDMS regions. For preparing the "rigid substrate", glass slides were first cleaned by a piranha solution (sulfuric acid to hydrogen peroxide (30%) = 3:1). HMDS was directly coated on the glass slide, and the following procedures for photolithography and FN/pluronic coating remained the same as for the soft substrate.

Nano-Indentation Measurement. The glass or PDMS substrates were cut with sharp blades and fixed for the measurement of their elastic constants by a Nano Indenter (Hysitron TI 950 TriboIndenter). The indentation modulus was calculated based on the reduced modulus $E_r = \frac{1}{2}\sqrt{\frac{\pi}{A}}\frac{dP}{dH}$, where A is the residual indentation area, and the maximum loading force dP and the depth of penetration dH were obtained by the unloading curve close to maximum load (Figure S1).

Cell Culture. Mouse fibroblasts (NIH-3T3) were cultured in Dulbecco's Modified Eagle's Medium mixed with Ham's F-12 in 1:1 ratio and supplemented with 10% fetal bovine serum and 1% penicillin/streptomycin. All cells were incubated at 37 °C in a humidified environment with supply of 5% CO_2 and 95% air. For the experiments with pharmacological inhibitors, cells were treated with 500 nM Latrunculin A (Sigma), 1 μM Cytochalasin D (Life Technology), 10 μM Y27632 (Alexis), or 2 μM Nocodazole (Sigma).

Fluorescence Labeling of Fixed Cells. Cells were seeded on micropatterned substrate at a density of 50 000 cells/cm^2, and then nonattaching cells were removed by refreshing the culture media after 30 min. Before acquiring the fluorescence images using a confocal microscope (Leica) or an inverted fluorescence microscope (Nikon), different fluorescence labeling procedures were applied according to the targeted intracellular components. To label only the nuclei, cells were incubated for 12 h, followed by applying 4% paraformaldehyde (PFA) for 15 min, 0.1% Triton X-100 for 10 min, and DAPI staining for 5 min. The sample was then mounted by Fluoromount G (Electon Microscopy Sciences. Inc.). To label simultaneously the pericentrin and nuclei for polarity analysis, cells were incubated for 12 h, followed by PBS washing and fixation using −30 °C methanol for 6 min. After drying, an Image-iT FX (Thermo Fisher Scientific) signal enhancer was applied for 30 min. Next, antipericentrin (1/500, Covance) was applied for 60 min, followed by application of antirabbit antibody (1/500, Thermo Fisher Scientific) for 30 min. The sample was rinsed with fresh PBS on a shaker for 5 min for 3 times between each change of solution. After that, cell nuclei were stained with DAPI for 5 min and mounted with Fluoromount G (Electon Microscopy Sciences. Inc.). To label the actin filaments, cells were fixed by 4% PFA for 15 min, followed by applying 0.1% Triton X-100 for 10 min and Image-iT FX signal enhancer (Life Technology) for 30 min. The actin filaments were then labeled with Rhodamine Phalloidin (1/40, Life Technology) for 1 h and mounted as aforementioned procedures. To analyze the actin distribution, images for cells on circular islands were stacked and averaged using Matlab. Specifically, Regionprops functions was used to crop and isolate individual cells. Using centroids of each cell for image registration, the images were stacked, and the intensity was normalized according to cell number. Heat map images were then generated referring to the grayscale level of fluorescence intensity to elucidate the distribution of actin.

Image Processing for Orientation Analysis. We implemented image processing in MATLAB to perform nucleus segmentation and measurement of long axis orientation of each nucleus with respect to the stripe boundary. The major challenge of the segmentation task was to separate individual nuclei from a cluster. We first applied Gaussian filter and thresholding on each raw microscopic image to obtain a binary image which shows clear regions of individual nuclei and nucleus clusters (Figure S2a). To differentiate individual nuclei and clusters, we further applied adaptive thresholding technique to generate a second binary image with a sharp boundary of each nucleus in a cluster (Figure S2b). These two binary images were combined using Boolean addition operation to obtain enhanced concave regions at the intersection points among nucleus boundaries (Figure S2c). Thus, the nucleus cluster can be identified by quantifying the concave region through checking the area difference between the actual region and its convex hull. Next, after identifying the cluster, the outmost pixels of each concave cluster were eliminated iteratively until the cluster was divided into more than one subregion. The same procedures were applied to each concave subregion until no concavity was detected. This method can segment all overlapping nuclei effectively and, despite the elimination of outmost layers, the shape characteristic of each nucleus was retained for orientation measurement. Finally, the long axis orientation of each nucleus was measured based on ellipse detection.

Live Nucleus Rotation and Cell Migration Analysis. The nuclei of live cells were stained with 2 μg/mL bisBenzimide H 33342 trihydrochloride (Sigma-Aldrich) and incubated at 37 °C in a humidified environment with supply of 5% CO_2 and 95% air for 30 min. Next, time-lapsed microscopy was conducted by an inverted microscope (Nikon) for 12 h with a 1 h interval. For dynamic analysis of cell orientation, the nucleus rotation was obtained based on the change of orientation angle between consecutive time-lapsed images. To determine the velocity of cell migration, we used the x-component of nucleus translocation velocity within a 1 h interval, and such velocity over the entire culture period of 12 h was averaged to represent the velocity of one cell.

Numerical Simulation. A two-dimensional coordinate system with an array of rods (10 rows × 30 columns) was built to represent the micropatterned stripes with cells inside. In this system, each rod represented the location and orientation of a single cell (Figure S3), which interacted and self-organized with the local orientation and the velocity gradient of cell migration. To simulate the velocity gradient of cell migration, a nonlinear velocity field with respect to the cell

DOI: 10.1021/acsami.6b06789
ACS Appl. Mater. Interfaces XXXX, XXX, XXX−XXX

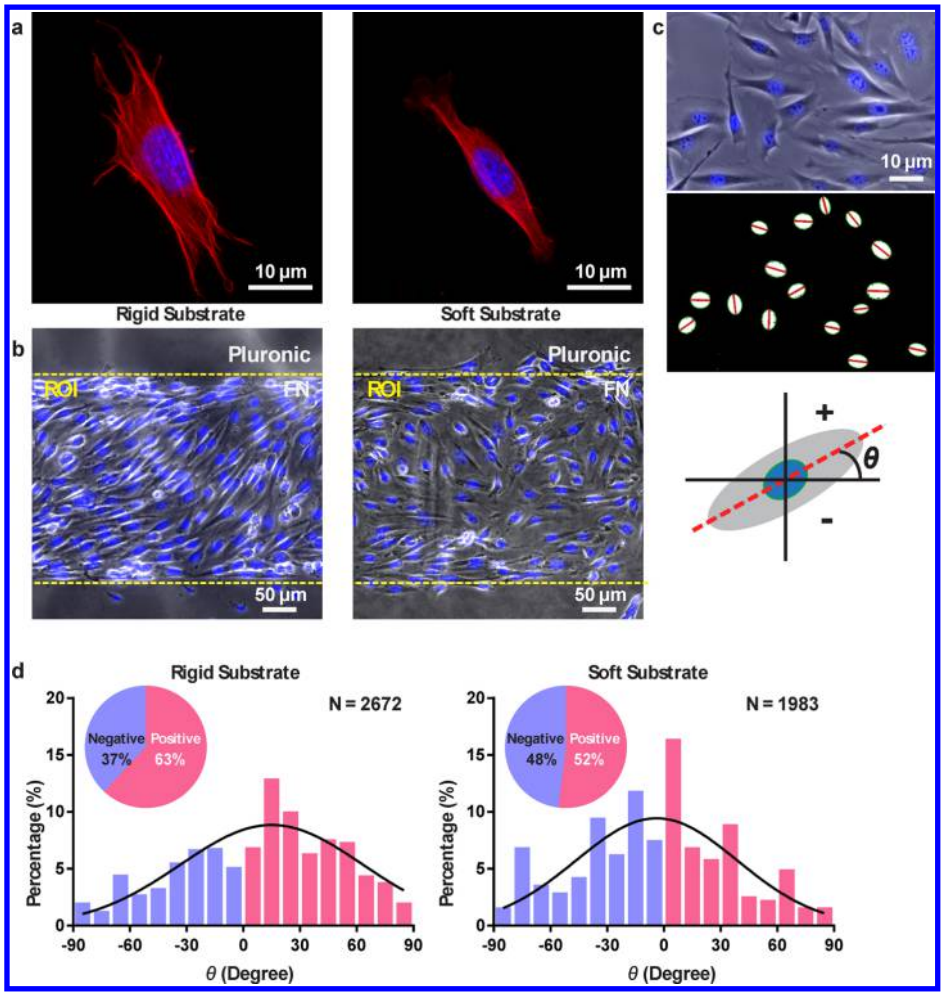

Figure 1. Left−right (LR) asymmetry of cell orientation on substrate with different stiffness. (a) Confocal microscopy showing the actin cytoskeleton of cells on rigid (glass) or soft (PDMS) substrate. (b) Phase contrast microscopy and DAPI stained nuclei showing the coherent orientation of cells cultured on alternating stripes of fibronectin (FN) and pluronic with different substrate stiffness. (c) Phase contrast microscopy and DAPI stained nuclei (upper) showing that the long axis of nuclei is aligned with the long axis of spindle-shaped cell. Using image processing (middle), the cell orientation can be determined by the orientation angle, θ, based on nucleus' long axis (lower). The θ is defined positive for counterclockwise (CCW) rotation and negative for clockwise (CW) rotation relative to the horizontally aligned stripe boundary. (d) Histogram of cell orientation of NIH 3T3 fibroblasts cultured on micropatterned stripes with different substrate stiffness.

location was formulated as $v = f(v_0, y, W) = v_0 \sin\left(\frac{\pi}{W} y\right)$, where y is the vertical coordinate with origin at center of the stripe, W is the total width of the stripe, and v_0 is the absolute migration velocity at stripe boundary. Note that this velocity gradient was not only used for cell translocation but also for cell rotation. When the cell orientation angle θ is greater than the average angle of its immediate 4 neighbors (upper, lower, left, and right) over a threshold, θ_0, that is, $\left|\theta - \frac{\theta_{upper} + \theta_{lower} + \theta_{left} + \theta_{right}}{4}\right| > \theta_0$ (Figure S4), we modeled the cell rotation as $\theta_{I+1} = \theta_I - k\frac{\Delta v \cdot \sin\theta}{R}$ (Figure S5), where I is the number of interaction, Δv is the velocity difference between the two termini of each rod, k is a scaling factor, and R is the length of the rod (set as 30 μm). All parameters were determined based on experimental observation (described in the Results section). On the basis of the formulation, the cell orientation and translocation were updated each iteration until the final pattern was stabilized (1 iteration = 1 h; total iterations = 10−15).

3. RESULTS

Cell Orientating with LR Asymmetry on Rigid Substrates, but Not on Soft Substrates. We first investigated whether the LR asymmetry of cell orientation is dependent on the substrate stiffness. We used parallel, micropatterned stripes of alternating coating of cell-adherent protein (fibronectin, FN) and cell-repellent molecules (pluronic). These parallel stripes were coated on glass slides as the rigid substrate (elastic modules = 65.6 ± 2.3 GPa) or PDMS as the soft substrate (elastic modules = 719.9 ± 48.8 KPa). Substrate stiffness can effectively alter the actomyosin organization and potentially the LR asymmetry of cells, as shown by the increased spreading area and enhanced actin filaments on rigid substrates (Figure 1a). After the seeded cells reached confluence on stripes (12 h), the LR asymmetry was analyzed based on the cell orientation relative to horizontally aligned stripe boundary (Figure 1b). The orientation angle, θ, was determined based on the long axis of nucleus related to the stripe boundary (Figure 1c), and was defined positive for counterclockwise (CCW) rotation with an acute angle and negative for clockwise (CW) rotation with an acute angle. Thus, if the LR asymmetry exists, the numbers of cells in positive or negative orientation would be unequal, and the mean angle of cell orientation would shift to nonzero. The results showed that, when cultured on the rigid substrate, 63%

DOI: 10.1021/acsami.6b06789
ACS Appl. Mater. Interfaces XXXX, XXX, XXX−XXX

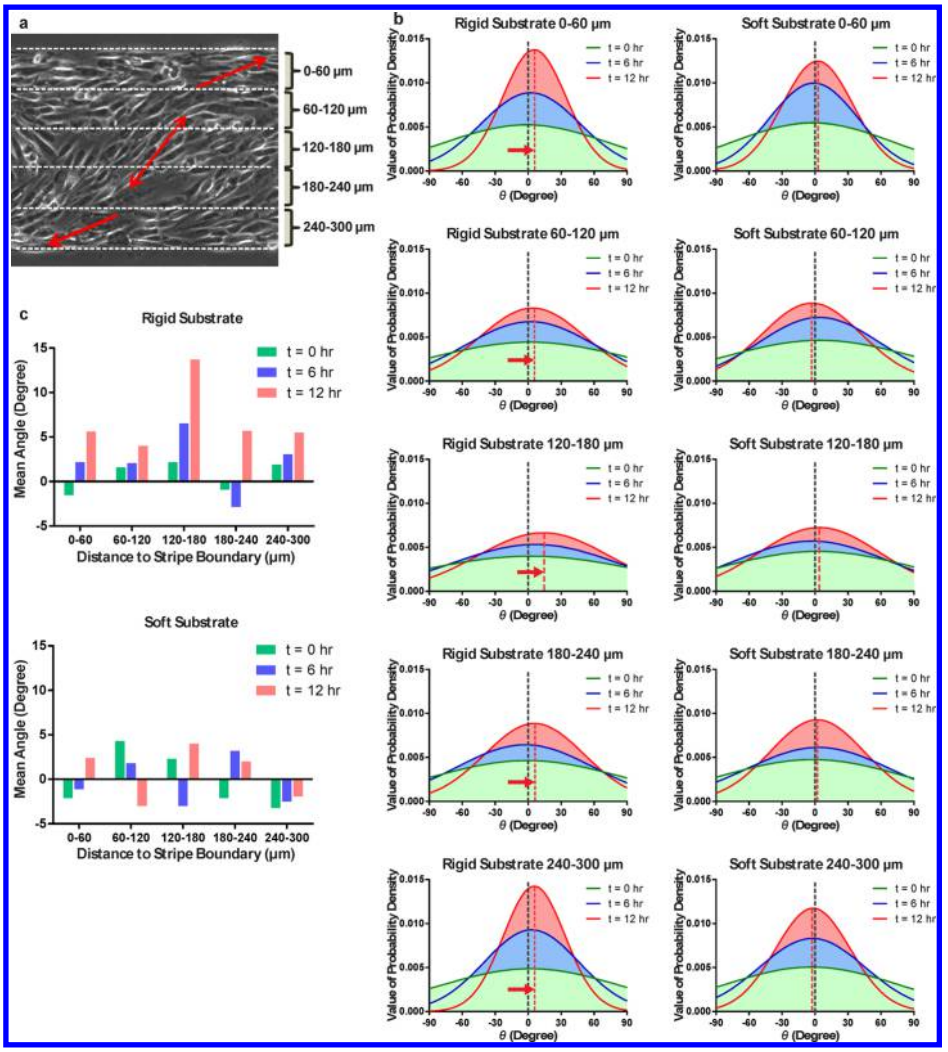

Figure 2. Dynamics of LR-biased cell orientation on substrate with different stiffness. (a) Schematic showing that the FN stripe was equally divided into 5 regions: 0−60, 60−120, 120−180, 180−240, and 240−300 μm. (b) Histogram of cell orientation in each region on rigid or soft substrate when t = 0, 6, or 12 h. The fitting curve was calculated based on a Gaussian function (total cell number for each curve fitting: $n > 1000$). (c) Mean angle of cell orientation in each region on rigid or soft substrate when t = 0, 6, or 12 h.

of cells showed a positive orientation, in which the average angle was 11.3° ± 0.6° (mean ± SEM; n = 2672) (Figure 1d). In contrast, when cultured on the soft substrate, the percentage of cells with positive orientation was reduced to 52%, and the average angle became 2.3° ± 0.8° (mean ± SEM; n = 1983; Figure 1d). This result suggests that cells exhibited significant LR-biased orientation when cultured on rigid substrates. More importantly, when a soft substrate was used, the cell orientation became collectively unbiased. Of note, although cells proliferated on both rigid and soft substrates, the difference between their density remained insignificant (Figure S6), which ruled out the potential influence by the difference of cell proliferation. Thus, because the only difference is substrate stiffness but not other factors (matrix protein, cell density, etc.), the result indicates that the substrate stiffness is key factor for the expression of cells' LR asymmetry.

Dynamics of LR-Biased Cell Orientation. To elucidate the developmental dynamics of the LR-biased cell orientation, we used live nucleus staining and time-lapsed microscopy. The orientations of live nuclei were averaged in 5 equally divided regions and continuously monitored for 12 h (Figure 2a). Immediately after plating, cell oriented randomly (green curve in Figure 2b). During the incubation process on rigid substrates, the cell orientation showed an increasing convergence from center to edge (blue and pink curve, Figure 2b), in which a highly coherent cell orientation was observed near the boundary (distance < 60 μm, Figure 2b). This coherent cell orientation is likely due to the preferred cell alignment along the stripe boundary and then propagated inward via an autocatalytic cell−cell alignment.[30] More importantly, when a rigid substrate was used, it caused a positive shift of the mean angle of cell orientation across different regions. Interestingly, the shift was the greatest for cells at the center region but not at the boundary (Figure 2b,c). In contrast, when cultured on soft substrates, while the increased convergence of cell orientation was also observed, which implied the existence of cell−cell alignment, the mean angle only fluctuated around zero degree, indicating that LR bias was completely abolished (Figure 2b,c). Together, we showed that the cell−cell and cell−boundary alignment was independent of substrate stiffness, and cells oriented with a positive mean angle on rigid substrates, in which the greatest angle was observed at the center of stripes.

Actin Distribution in Cells on Substrate with Different Stiffness. To understand how substrate stiffness regulates the

DOI: 10.1021/acsami.6b06789
ACS Appl. Mater. Interfaces XXXX, XXX, XXX−XXX

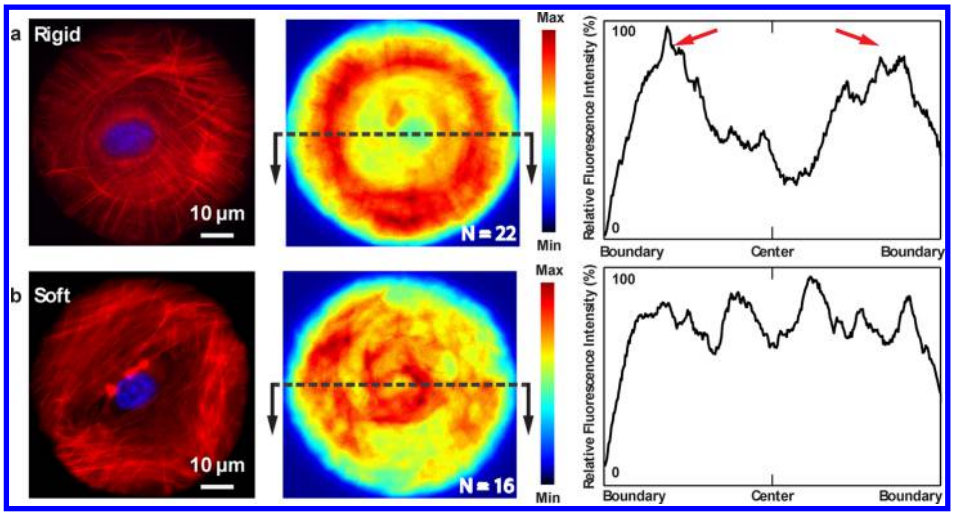

Figure 3. Actin distribution in cells on substrate with different stiffness. On (a) rigid substrate or (b) soft substrate, fluorescence microscopy images showing the actin distribution of cells on circular cell-adherent islands (left), the heat map of actin distribution after image stacking (middle), and the cross section curve of actin distribution of cells on circular islands (right). The dual peaks in the cross section curves showed the high intensity of actin ring on rigid substrates, whereas a relatively uniform distribution of fluorescence intensity suggested that the transverse arc was disorganized on soft substrates.

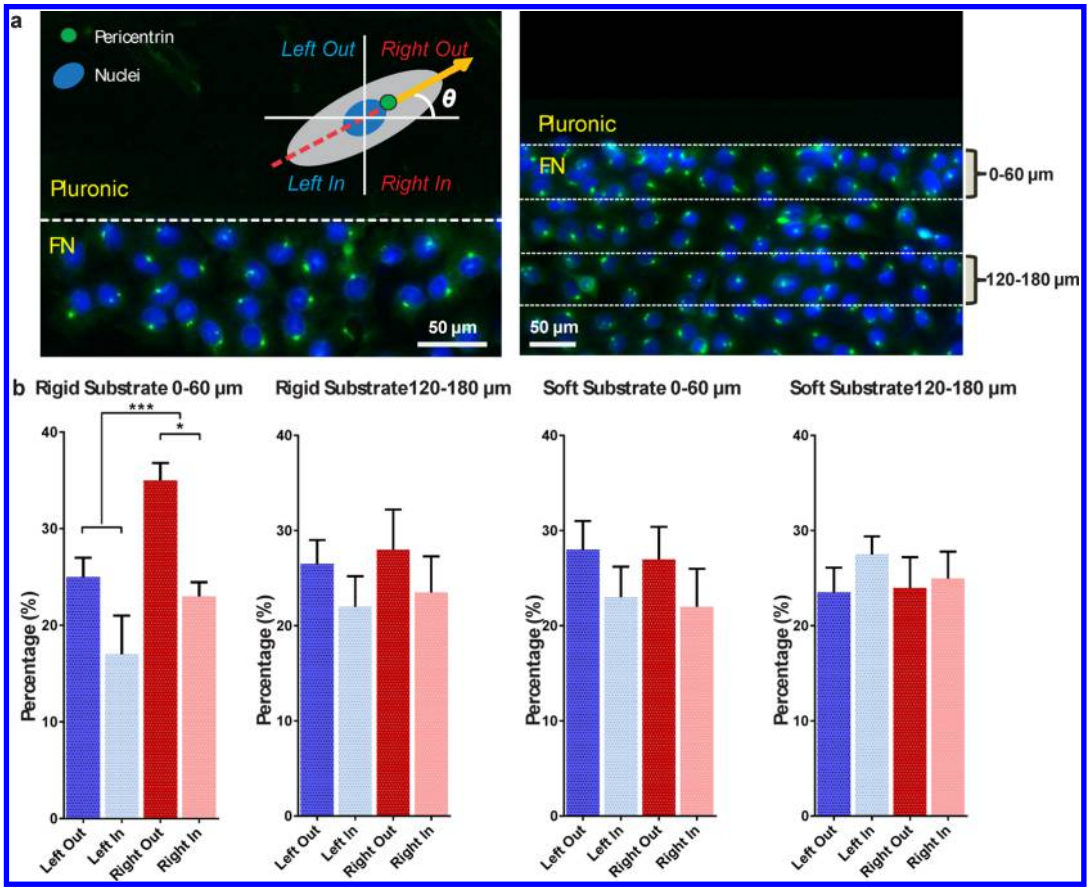

Figure 4. LR-biased cell polarity on substrate with different stiffness. (a) Schematic showing the classification of cell polarity. By orientating stripe boundary horizontally and placing the FN region at the lower half of the viewing zone, we classified the cell polarity according to the location of pericentrin (green) relative to the nucleus (blue) in quadrants of Right Out, Right In, Left Out, or Left In for cells adjacent to (0−60 μm) or distant from (120−180 μm) the stripe boundary. (b) Polarity of cells on substrate with different stiffness (mean ± SEM, quintuplicated experiment, total number of cells for at each region in each experiment: $n > 300$).

formation of LR-biased cell orientation, we first investigated the actin distribution. Actin is known to form a curved filament bundles, transverse arc, at the leading edge of a migrating cell.[31,32] Previous report showed that, when cultured on circular cell-adherent islands, transverse arcs would be in parallel with cell periphery, and its tangential movement along the island boundary is essential for the LR asymmetry of single cells.[16] As such, because reduced substrate stiffness was also known to

DOI: 10.1021/acsami.6b06789
ACS Appl. Mater. Interfaces XXXX, XXX, XXX−XXX

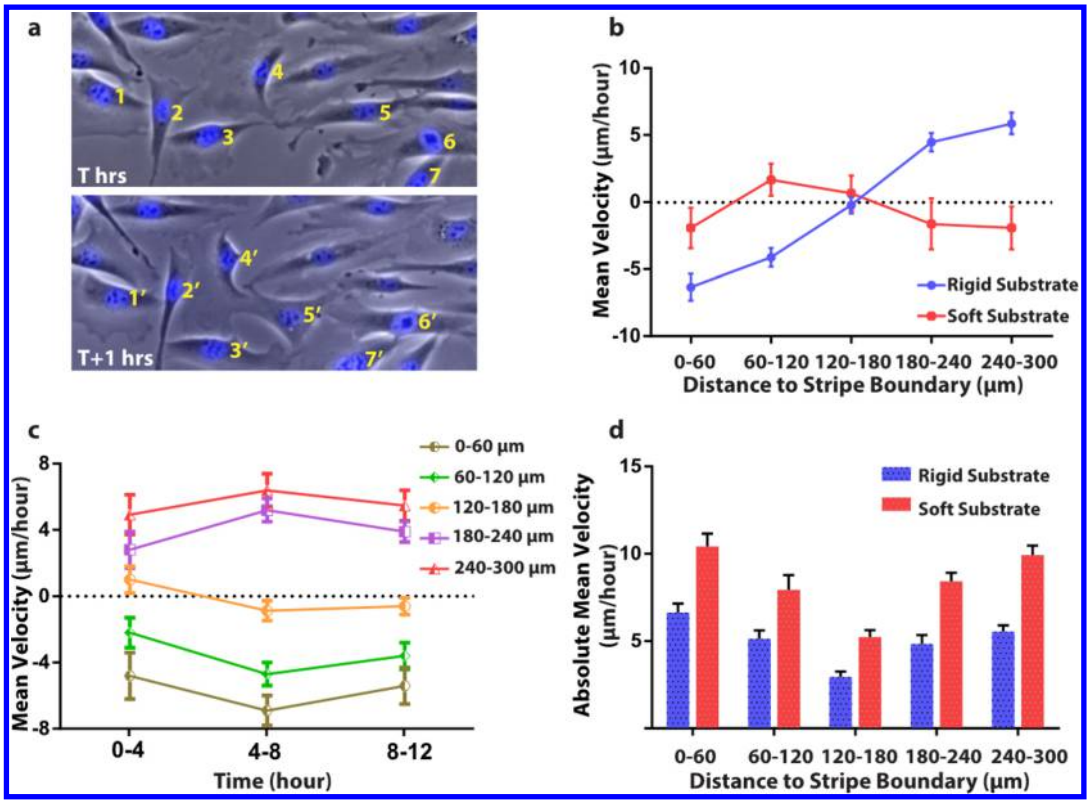

Figure 5. LR-biased cell migration on substrate with different stiffness. (a) Measurement of velocity of cell migration by the translocations of nuclei within 1 h interval. (b) Mean velocity of cell migration with respect to the distance to stripe boundary and substrate stiffness (mean ± SEM, quintuplicated experiment, total cell number at each region in each experiment: $n > 40$). Note that the rightward velocity is defined positive whereas the leftward velocity is negative. (c) On rigid substrates, the mean velocity of cell migration with respect to the distance to stripe boundary over time (mean ± SEM, quintuplicated experiment, total cell number at each region in each experiment: $n > 40$). (d) Absolute mean velocity of cell migration shown in panel b.

down-regulate the assembly of actin filaments,[33] the soft substrate may dissemble and disorganize the transverse arc, leading to the loss of LR asymmetry. To explore this possibility, we analyzed the actin distribution of cells on circular cell-adherent islands. After stacking multiple images of single cells, we found that actin formed a ring structure when cultured on rigid substrates, suggesting that the transverse arc was formed (Figure 3a). In contrast, on soft substrates, the actin was randomly distributed, suggesting that transverse arc was disorganized (Figure 3b). Thus, the stiffness regulates the configurations of transverse arc, which may account for the activation of LR bias.

LR-Biased Polarity on Substrate with Different Stiffness. We next studied the LR polarity when cultured on cell-adherent stripes. As aforementioned, the tangential shift of transverse arc along the micropatterned boundary is essential for the LR asymmetry. Thus, when cultured on unbiased micropatterned stripes, this tangential shift along the stripe boundary could also drive cells to polarize and migrate along the stripe boundary with LR bias. The direction of cell migration is mediated by polarization of intracellular apparatus,[34] which can be viewed by the location of pericentrin relative to the nucleus. By orientating stripes horizontally and placing the FN region at the lower half of the viewing zone, we classified the polarity by pericentrin location relative to nucleus centroid in quadrants of Left Out, Left In, Right Out, and Right In (Figure 4a). The result showed that cells cultured on rigid substrates close to the boundary (distance = 0−60 μm) exhibited a clear right/out bias (Figure 4b), suggesting that cells inside the FN stripes were migrating outward with a rightward bias. Moreover, such bias was attenuated for cells located in remote regions (distance = 120−180 μm), indicating that LR polarity was only activated in cells near the stripe boundary. In contrast, for cells cultured on soft substrates, such LR bias was abolished regardless of the location of cells. Thus, it suggests that the LR-biased cell orientation on rigid substrates might be associated with the appearance of transverse arc which regulates the LR-biased polarization and migration, and such LR bias can be activated or deactivated depending on substrate stiffness.

LR-Based Cell Migration on Substrate with Different Stiffness. To validate further that the LR-biased migration indeed participated in the development of LR-biased orientation, we directly measured the velocity of cell migration based on the translocation of stained nuclei in live cells (Figure 5a). We measured the x-component of nucleus translocation during the time-lapsed monitoring (total 12 h with 1 h interval), and the velocity of each hour was averaged to represent the velocity of that single cell. On rigid substrates, we found that when cells were near the stripe boundary, cells migrated with a strong rightward bias (Figure 5b). Such LR bias of cell migration grew over time, and decayed when cells were distant from the boundary (Figure 5c). However, when cultured on soft substrates, no significant LR bias was observed (Figure 5b). Moreover, the absolute velocity showed cell migrated faster than that on rigid substrates (Figure 5d). Together, our results demonstrate that the velocity gradient of cell migration within the FN stripes may be the underlying mechanism of this stiffness-dependent LR asymmetry. For cells

DOI: 10.1021/acsami.6b06789
ACS Appl. Mater. Interfaces XXXX, XXX, XXX−XXX

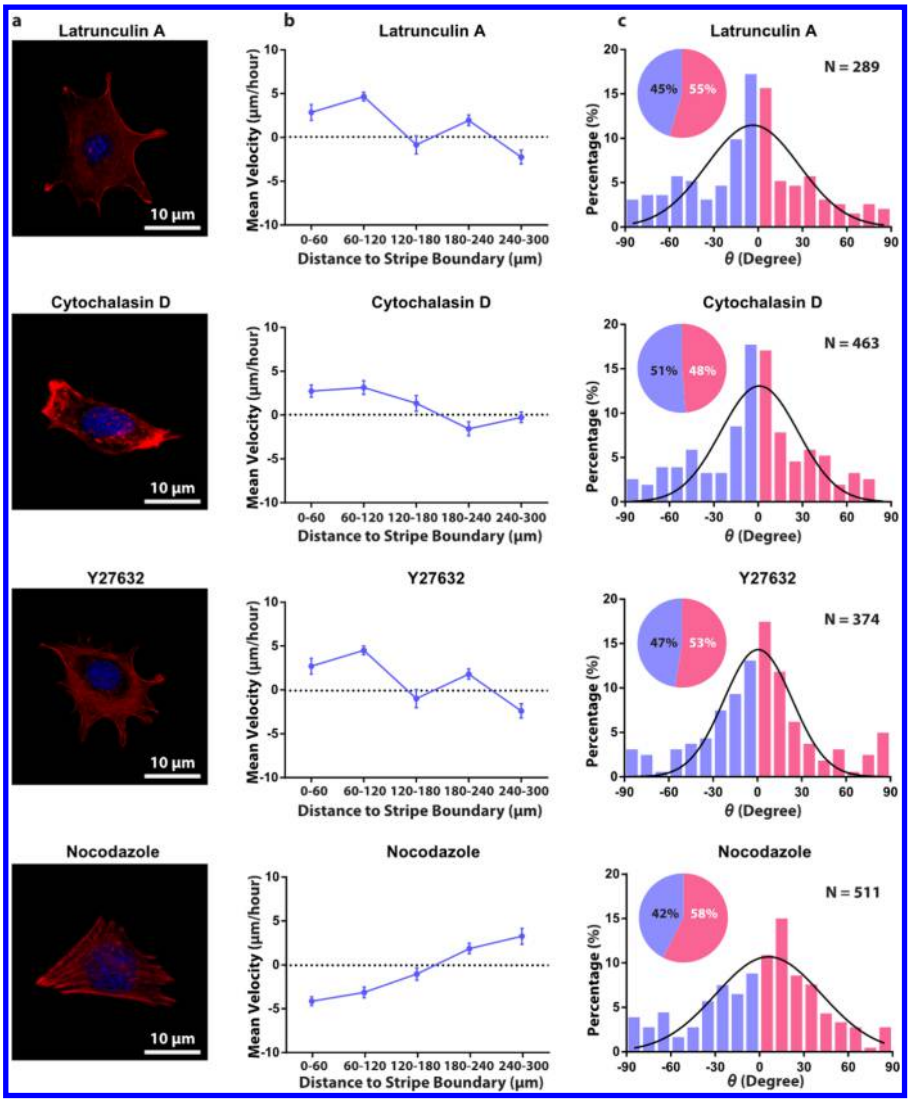

Figure 6. Actin cytoskeleton, LR-biased cell migration, and LR-biased cell orientation on rigid substrates with actin inhibitors. (a) Confocal microscopy showing the actin cytoskeleton of cells with different treatment. (b) Mean velocity of cell migration with respect to the distance to stripe boundary and different treatment (mean ± SEM, quintuplicated experiment, total cell number at each region in each experiment: $n > 40$). (c) Histogram of cell orientation with different treatment.

on soft substrates, the faster but unbiased velocity may only randomize the cell orientation.

Inhibition of Actin Cytoskeleton. To validate further the role of actin in this stiffness-dependent LR bias, we applied actin inhibitors for cells on rigid substrates. It was noted that, when cultured on soft substrates, the LR bias of cell polarity and migration was abolished (Figures 4 and 5), and the absolute velocity was indeed increased (Figure 5d). As the soft substrate was known to disorganize the formation of transverse arc (Figure 3), possibly due to the down-regulation of actin filaments,[33] the unbiased and faster cell migration on soft substrates may be also mediated by the disassembly of actin stress fiber. To explore this possibility, we applied actin inhibitors, Latrunculin A, Cytochalasin D, and Y27632, to cells on rigid substrates to suppress the assembly of actin filaments (Figure 6a). Latrunculin A and Cytochalasin D prevent the combination of F-actin and G-actin, therefore inhibiting actin polymerization.[35,36] Y27632 inhibits the upstream Rho-associated kinase (ROCK), thereby preventing the formation of actin stress fiber.[37] The result showed that cell treated with Latrunculin A, Cytochalasin D, or Y27632 expressed an unbiased and faster migration (Figure 6b and Figure S7), eventually resulting in an unbiased cells orientation (Figure 6c). Remarkably, the observed cell behaviors when treated with actin inhibitors were similar to that on soft substrates, suggesting that the down-regulation of actin filaments by either chemical (actin inhibitor) or mechanical (substrate stiffness) methods could be the ultimate cause of the unbiased and faster migration. To confirm further the role of actin stress fiber, we used Nocodazole, which interferes the polymerization of microtubules but not the assembly of actin filaments (Figure 6a).[8] The result showed that the LR-biased velocity gradient and cell orientation were still observed (Figure 6b,c), and the absolute velocity only slightly increased (Figure S7). Thus, the result collectively suggested that the assembly of actin filaments should be crucial for the formation of LR asymmetry, and a rigid substrate should be required in activating the process.

Numerical Simulation. To elucidate how LR-biased velocity gradient can lead to the LR-biased cell orientation, we applied numerical simulation. The analysis of cell migration

DOI: 10.1021/acsami.6b06789
ACS Appl. Mater. Interfaces XXXX, XXX, XXX−XXX

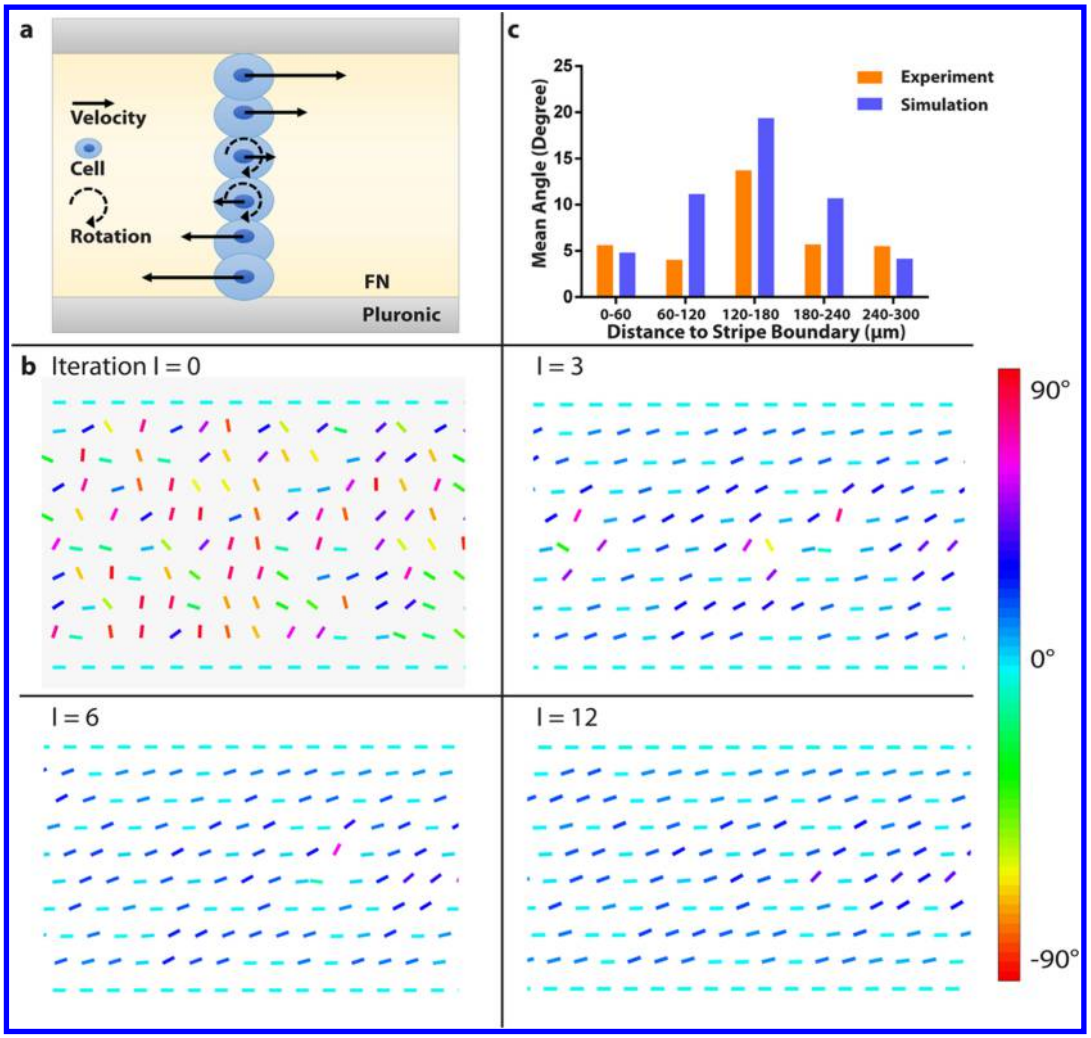

Figure 7. Numerical simulation showing the propagation of LR-biased orientation via the velocity gradient of cell migration. (a) Illustration of simulated cell movement. (b) Each rod represents individual cell with its own location and orientation, where the colors represent the orientation angle corresponding to color bar at the right. A random distribution is set at $I = 0$. With more iteration ($I > 1$), increasing convergence of cell orientation was establishes in cells adjacent to stripe boundary and then propagates to distant area via cell rotation. (c) Mean angle of cell orientation in each region acquired from experiment and simulation.

suggested that the LR-biased migration might underlie the formation of LR-biased orientation. However, how the LR-biased migration can lead to a greater orientation angle at the center region remains puzzling (Figure 2b,c). To answer this question, an array of rotating rod was built to represent the locations and orientations of cells cultured on micropatterned stripes. We modeled the cell movement including (1) cell migration, (2) cells' local alignment with the neighboring cells, and (3) cell rotation based on the velocity gradient of cell migration (Figure 7a). On the basis of the measured cell migration (Figure 5b), the velocity profile was formulated as $v = v_0 \sin\left(\frac{\pi}{W} y\right)$, where the absolute migration velocity at stripe boundary, v_0, was set as 6 μm/h according to the experimental result (Figure 5b and Figure S8). To model the local alignment, the orientation angle of each rod, θ, was compared with its immediate 4 neighbors (Figure S4). If the angular difference was below a threshold, θ_0, the θ was kept unchanged. On the contrary, if the angular difference was over θ_0, the θ was updated following the equation, $\theta_{I+1} = \theta_I - k\frac{\Delta v \cdot \sin\theta}{R}$ (see Experimental Section and SI for details). The threshold θ_0 was set as 20° according to the absolute angle difference between two adjacent cells along the y-axis of the stripe, i.e., 22.54° ± 21.02° (mean ± STD; $n = 119$). The scaling factor k was set as 167, which was experimentally determined based on the location, orientation θ, and the angular velocity of nuclei (167.41 ± 202.6, mean ± STD; $n = 52$). A random distribution was generated at iteration $I = 0$ to simulate the randomized cell orientation immediately after plating, whereas the orientation of cells at the stripe boundary was maintained horizontal based on the preferred cell alignment along the stripe boundary (Figure 2b and Figure 7b). With time, cells moved following the velocity field, aligned with their neighbors and with the stripe boundary, and rotated due to the velocity gradient. After a number of iterations, we found that a LR-biased orientation was formed with more coherent orientation (Figure 7b). With more iterations, the LR-biased orientation patterns appeared similar to the experimental observation (Figure 7b and Figure 1b). Notably, for the cells close to the boundary, increased convergence of cell orientation was observed. More importantly, while less coherent, the positive shift in the mean angle of cell orientation was the greatest for the cells at the center region, which is consistent with the experimental observation

DOI: 10.1021/acsami.6b06789
ACS Appl. Mater. Interfaces XXXX, XXX, XXX−XXX

(Figure 7c). In this simulation, LR-biased orientation was clearly seen, which demonstrates how velocity field regulates the propagation of LR-biased cell orientation.

4. DISCUSSION

Substrate stiffness regulates cell behavior in various aspects, whereas its influence on the development of LR asymmetry has been rarely addressed. Here, using micropatterned cell-adherent stripes on substrate with different stiffness, our assay reveals that substrate stiffness regulates the formation of LR asymmetry. We found that, on rigid substrates, cells at stripe boundary polarized and migrated with LR bias. Such LR-biased mechanics subsequently propagated to the cells remote from the boundary, leading to a LR-biased cell orientation in multicellular organization. In contrast, for cells cultured on soft substrates, the LR-biased mechanics (polarity, migration, and orientation) were all abrogated. Further characterization shows that the dependence of LR asymmetry could be associated with the assembly of actin filaments and the formation of transverse arc on rigid substrates. To our knowledge, it is the first demonstration showing how substrate stiffness influences the LR mechanics being unfolded from single cells to the LR feature in multicellular organization. Because different tissues and organs may have different stiffness ranging from 10 to 2000 kPa, our result suggests that cells may be encoded with varied LR bias that reacts to the change of cell−matrix interaction in different manner, which eventually leads to the characteristic orientation and proper formation of tissue architectures. Thus, with an in-depth understanding of LR asymmetry formation, our result suggests substrate stiffness as an effective regulator in reproducing the LR asymmetry in tissue development.

The NIH 3T3 fibroblasts migrated with rightward bias depending on substrate stiffness, in which the assembly/disassembly of actin filaments may be the key mediator. Assembly of actin stress fibers has been demonstrated as the prerequisite to generate cellular LR bias.[11,13] Report showed that a chiral pattern of two classes of actin filaments, transverse arc and radial fibers in single cell, might be the ultimate origin underlying the LR bias.[16] That is, when cells were cultured on circular cell-adherent islands, the transverse arc produces a unidirectional, tangential shift along the micropatterned boundary, by which the chirality can be characterized by the tilted orientation of dorsal stress fibers.[16] It indicates that the tangential shift of transverse arc could be the key underlying the LR-biased mechanics of single cells, and rigid substrate is required for the formation of transverse arc (Figure 3). Moreover, the cellular LR asymmetry is phenotype-dependent, i.e., NIH 3T3 fibroblasts exhibited rightward bias, whereas C2C12 myoblasts exhibited leftward bias.[8] Consistent with the previous reports, the rightward direction of NIH 3T3 fibroblast was also observed in our results. Although the mechanism is not fully understood, we speculate that the chiral alignment of actin filaments may vary in different forms from one cell type to another. Thus, the LR-biased migration and orientation are the consequence on account of cell type and stiffness.

It remains unclear how LR-biased cell migration was induced by the tangential shift of transverse arc of individual cells. When cultured on unbiased micropatterned stripes of cell-adherent substrates, it has been reported that cells at stripe boundary would polarize themselves to "face" outward to the unoccupied regions.[38] Meanwhile, because of the boundary constrains, cells at the stripe boundary would assemble additional actin stress fibers, which is also known essential for the LR asymmetry.[11] As such, we speculate that the tangential shift of transverse arc along the stripe boundary may participate the assembling process of stress fibers, which subsequently drives a lateral shift of intracellular apparatus and eventually lead to the cell polarity with LR bias.

We found that cells treated with actin inhibitors exhibited a depolymerized actin stress fiber, which was accompanying with a faster but unbiased migration. This phenomenon was also observed in cells on soft substrates. Associated with polymerization of actin cytoskeleton, focal adhesion mediates cell migration velocity through its strength and exterior anchorage on extracellular matrix.[39] Mature focal adhesions are postulated as the "brake" on the cell migration machinery. Thus, the increased cell motility may presumably through the promotion of focal adhesion turnover and reduction of focal adhesion at center of cells, which then enable cells to migrate faster and more directional.[40,41]

In the formation of LR asymmetry in multicellular organization, our numerical simulation showed that the propagation of LR asymmetry was through a cell rotation in response to the LR-biased velocity gradient. It indicates that an intercellular force transmission might be involved. As reported by others, cadherin plays an important role in the propagation of LR asymmetry,[42] in which the disruption of transmembrane cadherin destroyed the asymmetric velocity profile on stripe and then broke the LR-biased orientation. Thus, the propagation of LR bias via velocity gradient of cells on rigid substrates may be also due to the cadherin-mediated force transmission between cells.

5. CONCLUSIONS

In summary, this work suggests that substrate stiffness can function as an effective regulator for the formation and propagation of LR asymmetry. The LR asymmetry was initiated by a LR-biased migration of cells at stripe boundary, which later generated a velocity gradient propagating inward, eventually leading to a coherent LR-biased cell orientation over the entire cell layer. This self-organized LR asymmetry requires a sufficient level of substrate rigidity, possibly because soft substrate would down-regulate the assembly of actin filaments and neutralize the LR bias. Together, these findings deepen our understandings of how to reproduce and regulate the LR asymmetry in an engineered context, paving ways for further studies of cell mechanics, and regeneration of missing or injured tissues in the future.

■ ASSOCIATED CONTENT

Supporting Information

The Supporting Information is available free of charge on the ACS Publications website at DOI: 10.1021/acsami.6b06789.

Load-depth curve of Nano-Indentation, image segmentation for orientation analysis, schematic of the assay of rods simulating the location and orientation of cells, schematic illustration showing the local alignment of an orientation angle θ with its immediate neighbors, schematic illustration showing the simulated cell rotation by a velocity gradient, the cell density on rigid or soft substrate when cultured on micropatterned stripes, the absolute mean velocity of nontreated cells on different substrate stiffness and cells on rigid substrates treated with actin inhibitor, the mean velocity from experiment and velocity profile used in the simulation (PDF).

DOI: 10.1021/acsami.6b06789
ACS Appl. Mater. Interfaces XXXX, XXX, XXX−XXX

AUTHOR INFORMATION

Corresponding Authors

*M. L. Lam. Email: miu.lam@cityu.edu.hk.
*T.-H. Chen. Email: thchen@cityu.edu.hk.

Notes

The authors declare no competing financial interest.

ACKNOWLEDGMENTS

We acknowledge the support from the National Natural Science Foundation of China (Grant No. 51305375), Early Career Scheme of Hong Kong Research Grants Council (Grant No. 21214815), Croucher Foundation (Grant No. 9500016), and the Science Technology and Innovation Committee of Shenzhen Municipality (Grant No. JCYJ20150601102053061).

REFERENCES

(1) Aw, S.; Levin, M. What's Left in Asymmetry? *Dev. Dyn.* **2008**, *237*, 3453−3463.
(2) Lobikin, M.; Wang, G.; Xu, J. S.; Hsieh, Y. W.; Chuang, C. F.; Lemire, J. M.; Levin, M. Early, Nonciliary Role for Microtubule Proteins in Left-Right Patterning Is Conserved Across Kingdoms. *Proc. Natl. Acad. Sci. U. S. A.* **2012**, *109*, 12586−12591.
(3) Veerkamp, J.; Rudolph, F.; Cseresnyes, Z.; Priller, F.; Otten, C.; Renz, M.; Schaefer, L.; Abdelilah-Seyfried, S. Unilateral Dampening of Bmp Activity by Nodal Generates Cardiac Left-Right Asymmetry. *Dev. Cell* **2013**, *24*, 660−667.
(4) Streeter, D. D., Jr; Spotnitz, H. M.; Patel, D. P.; Ross, J., Jr; Sonnenblick, E. H. Fiber Orientation in the Canine Left Ventricle During Diastole and Systole. *Circ. Res.* **1969**, *24*, 339−347.
(5) Xu, J. S.; Van Keymeulen, A.; Wakida, N. M.; Carlton, P.; Berns, M. W.; Bourne, H. R. Polarity Reveals Intrinsic Cell Chirality. *Proc. Natl. Acad. Sci. U. S. A.* **2007**, *104*, 9296−9300.
(6) Pohl, C.; Bao, Z. R. Chiral Forces Organize Left-Right Patterning in C. Elegans by Uncoupling Midline and Anteroposterior Axis. *Dev. Cell* **2010**, *19*, 402−412.
(7) Danilchik, M. V.; Brown, E. E.; Riegert, K. Intrinsic Chiral Properties of the Xenopus Egg Cortex: An Early Indicator of Left-Right Asymmetry? *Development* **2006**, *133*, 4517−4526.
(8) Wan, L. Q.; Ronaldson, K.; Park, M.; Taylor, G.; Zhang, Y.; Gimble, J. M.; Vunjak-Novakovic, G. Micropatterned Mammalian Cells Exhibit Phenotype-Specific Left-Right Asymmetry. *Proc. Natl. Acad. Sci. U. S. A.* **2011**, *108*, 12295−12300.
(9) Chen, T. H.; Zhu, X. L.; Pan, L. T.; Zeng, X. J.; Garfinkel, A.; Tintut, Y.; Demer, L. L.; Zhao, X.; Ho, C. M. Directing Tissue Morphogenesis via Self-Assembly of Vascular Mesenchymal Cells. *Biomaterials* **2012**, *33*, 9019−9026.
(10) Singh, A. V.; Mehta, K. K.; Worley, K.; Dordick, J. S.; Kane, R. S.; Wan, L. Q. Carbon Nanotube-Induced Loss of Multicellular Chirality on Micropatterned Substrate Is Mediated by Oxidative Stress. *ACS Nano* **2014**, *8*, 2196−2205.
(11) Chen, T. H.; Hsu, J. J.; Zhao, X.; Guo, C. Y.; Wong, M. N.; Huang, Y.; Li, Z. W.; Garfinkel, A.; Ho, C. M.; Tintut, Y.; Demer, L. L. Left-Right Symmetry Breaking in Tissue Morphogenesis via Cytoskeletal Mechanics. *Circ. Res.* **2012**, *110*, 551−559.
(12) Taniguchi, K.; Maeda, R.; Ando, T.; Okumura, T.; Nakazawa, N.; Hatori, R.; Nakamura, M.; Hozumi, S.; Fujiwara, H.; Matsuno, K. Chirality in Planar Cell Shape Contributes to Left-Right Asymmetric Epithelial Morphogenesis. *Science* **2011**, *333*, 339−341.
(13) Noël, E. S.; Verhoeven, M.; Lagendijk, A. K.; Tessadori, F.; Smith, K.; Choorapoikayil, S.; den Hertog, J.; Bakkers, J. A Nodal-Independent and Tissue-Intrinsic Mechanism Controls Heart-Looping Chirality. *Nat. Commun.* **2013**, *4*, doi: 10.1038/ncomms3754.
(14) Hozumi, S.; Maeda, R.; Taniguchi, K.; Kanai, M.; Shirakabe, S.; Sasamura, T.; Spéder, P.; Noselli, S.; Aigaki, T.; Murakami, R.; Matsuno, K. An Unconventional Myosin in Drosophila Reverses the Default Handedness in Visceral Organs. *Nature* **2006**, *440*, 798−802.
(15) Spéder, P.; Adám, G.; Noselli, S. Type ID Unconventional Myosin Controls Left-Right Asymmetry in Drosophila. *Nature* **2006**, *440*, 803−807.
(16) Tee, Y. H.; Shemesh, T.; Thiagarajan, V.; Hariadi, R. F.; Anderson, K. L.; Page, C.; Volkmann, N.; Hanein, D.; Sivaramakrishnan, S.; Kozlov, M. M.; Bershadsky, A. D. Cellular Chirality Arising from the Self-Organization of the Actin Cytoskeleton. *Nat. Cell Biol.* **2015**, *17*, 445−457.
(17) Discher, D. E.; Janmey, P. A.; Wang, Y. L. Tissue Cells Feel and Respond to the Stiffness of Their Substrate. *Science* **2005**, *310*, 1139−1143.
(18) Wang, Y.; Wang, G. X.; Luo, X. D.; Qiu, J. H.; Tang, C. J. Substrate Stiffness Regulates the Proliferation, Migration, and Differentiation of Epidermal Cells. *Burns* **2012**, *38*, 414−420.
(19) Lam, R. H. W.; Sun, Y. B.; Chen, W. Q.; Fu, J. P. Elastomeric Microposts Integrated into Microfluidics for Flow-Mediated Endothelial Mechanotransduction Analysis. *Lab Chip* **2012**, *12*, 1865−1873.
(20) Obi, S.; Masuda, H.; Shizuno, T.; Sato, A.; Yamamoto, K.; Ando, J.; Abe, Y.; Asahara, T. Fluid Shear Stress Induces Differentiation of Circulating Phenotype Endothelial Progenitor Cells. *Am. J. Physiol. Cell Physiol.* **2012**, *303*, C595−C606.
(21) Guo, W. H.; Frey, M. T.; Burnham, N. A.; Wang, Y. L. Substrate Rigidity Regulates the Formation and Maintenance of Tissues. *Biophys. J.* **2006**, *90*, 2213−2220.
(22) Dokukina, I. V.; Gracheva, M. E. A Model of Fibroblast Motility on Substrates with Different Rigidities. *Biophys. J.* **2010**, *98*, 2794−2803.
(23) Engler, A. J.; Griffin, M. A.; Sen, S.; Bönnemann, C. G.; Sweeney, H. L.; Discher, D. E. Myotubes Differentiate Optimally on Substrates with Tissue-Like Stiffness: Pathological Implications for Soft or Stiff Microenvironments. *J. Cell Biol.* **2004**, *166*, 877−887.
(24) Engler, A. J.; Sen, S.; Sweeney, H. L.; Discher, D. E. Matrix Elasticity Directs Stem Cell Lineage Specification. *Cell* **2006**, *126*, 677−689.
(25) Even-Ram, S.; Artym, V.; Yamada, K. M. Matrix Control of Stem Cell Fate. *Cell* **2006**, *126*, 645−647.
(26) Guilak, F.; Cohen, D. M.; Estes, B. T.; Gimble, J. M.; Liedtke, W.; Chen, C. S. Control of Stem Cell Fate by Physical Interactions with the Extracellular Matrix. *Cell Stem Cell* **2009**, *5*, 17−26.
(27) Sniadecki, N. J.; Anguelouch, A.; Yang, M. T.; Lamb, C. M.; Liu, Z.; Kirschner, S. B.; Liu, Y.; Reich, D. H.; Chen, C. S. Magnetic Microposts as an Approach to Apply Forces to Living Cells. *Proc. Natl. Acad. Sci. U. S. A.* **2007**, *104*, 14553−14558.
(28) Tan, J. L.; Tien, J.; Pirone, D. M.; Gray, D. S.; Bhadriraju, K.; Chen, C. S. Cells Lying on a Bed of Microneedles: An Approach to Isolate Mechanical Force. *Proc. Natl. Acad. Sci. U. S. A.* **2003**, *100*, 1484−1489.
(29) Fu, J. P.; Wang, Y. K.; Yang, M. T.; Desai, R. A.; Yu, X. A.; Liu, Z. J.; Chen, C. S. Mechanical Regulation of Cell Function with Geometrically Modulated Elastomeric Substrates. *Nat. Methods* **2010**, *7*, 733−736.
(30) Junkin, M.; Leung, S. L.; Whitman, S.; Gregorio, C. C.; Wong, P. K. Cellular Self-Organization by Autocatalytic Alignment Feedback. *J. Cell Sci.* **2011**, *124*, 4213−4220.
(31) Hotulainen, P.; Lappalainen, P. Stress fibers are generated by two distinct actin assembly mechanisms in motile cells. *J. Cell Biol.* **2006**, *173*, 383−394.
(32) Tojkander, S.; Gateva, G.; Lappalainen, P. Actin Stress Fibers - Assembly, Dynamics and Biological Roles. *J. Cell Sci.* **2012**, *125*, 1855−1864.
(33) Yeung, T.; Georges, P. C.; Flanagan, L. A.; Marg, B.; Ortiz, M.; Funaki, M.; Zahir, N.; Ming, W.; Weaver, V.; Janmey, P. A. Effects of Substrate Stiffness on Cell Morphology, Cytoskeletal Structure, and Adhesion. *Cell Motil. Cytoskeleton* **2005**, *60*, 24−34.
(34) Ridley, A. J.; Schwartz, M. A.; Burridge, K.; Firtel, R. A.; Ginsberg, M. H.; Borisy, G.; Parsons, J. T.; Horwitz, A. R. Cell Migration: Integrating Signals from Front to Back. *Science* **2003**, *302*, 1704−1709.

DOI: 10.1021/acsami.6b06789
ACS Appl. Mater. Interfaces XXXX, XXX, XXX−XXX

(35) Coué, M.; Brenner, S. L.; Spector, I.; Korn, E. D. Inhibition of Actin Polymerization by Latrunculin A. *FEBS Lett.* **1987**, *213*, 316−318.
(36) Cooper, J. A. Effects of Cytochalasin and Phalloidin on Actin. *J. Cell Biol.* **1987**, *105*, 1473−1478.
(37) Ishizaki, T.; Uehata, M.; Tamechika, I.; Keel, J.; Nonomura, K.; Maekawa, M.; Narumiya, S. Pharmacological Properties of Y-27632, A Specific Inhibitor of Rho-Associated Kinases. *Mol. Pharmacol.* **2000**, *57*, 976−983.
(38) Desai, R. A.; Gao, L.; Raghavan, S.; Liu, W. F.; Chen, C. S. Cell Polarity Triggered by Cell-Cell Adhesion via E-Cadherin. *J. Cell Sci.* **2009**, *122*, 905−911.
(39) Gupton, S. L.; Waterman-Storer, C. M. Spatiotemporal Feedback Between Actomyosin and Focal-Adhesion Systems Optimizes Rapid Cell Migration. *Cell* **2006**, *125*, 1361−1374.
(40) Conti, M. A.; Adelstein, R. S. Nonmuscle Myosin II Moves in New Directions. *J. Cell Sci.* **2008**, *121*, 11−18.
(41) Totsukawa, G.; Wu, Y.; Sasaki, Y.; Hartshorne, D. J.; Yamakita, Y.; Yamashiro, S.; Matsumura, F. Distinct Roles of MLCK and Rock in the Regulation of Membrane Protrusions and Focal Adhesion Dynamics During Cell Migration of Fibroblasts. *J. Cell Biol.* **2004**, *164*, 427−439.
(42) Worley, K. E.; Shieh, D.; Wan, L. Q. Inhibition of Cell-Cell Adhesion Impairs Directional Epithelial Migration on Micropatterned Surfaces. *Integr. Biol.* **2015**, *7*, 580−590.

DOI: 10.1021/acsami.6b06789
ACS Appl. Mater. Interfaces XXXX, XXX, XXX−XXX